IMPULSIVE PENETRATION OF SOLAR WIND PLASMA IRREGULARITIES INTO THE MAGNETOSPHERE : RELEVANT LABORATORY EXPERIMENTS.

J. LEMAIRE *
DESPA, Observatoire de Meudon, France.

ABSTRACT. Before detailed high resolution and multi-point observations of the magnetopause region will become available in the 90's, it is interesting to reexamine existing Controlled Laboratory Plasma Experiments which are relevant to the study of solar wind - magnetosphere interaction. Two series of such laboratory experiments have been reviewed in this article. Their application to the solar wind - magnetosphere system has been presented and discussed. But other additional laboratory experiments exist; they should also be reconsidered and possibly extended.

1. What can we learn from laboratory experiments?

Before CLUSTER's detailed in-situ observations will become available to the science community in the 90's, it can be quite instructive to examine available Laboratory Plasma Experiments which are relevant to our topic.

The purpose of this paper is precisely to review two sets of laboratory plasma experiments which are mostly unknown or overlooked by a large fraction of our space science community. We will show below to which extent these basic plasma physics experiments are relevant for the study of solar wind-magnetosphere interaction.

* *On leave of absence from, IASB, 3, av. Circulaire, B-1180, Brussels, Belgium*

P. E. Sandholt and A. Egeland (eds.), Electromagnetic Coupling in the Polar Clefts and Caps, 27–42.

The first set of these experiments is that of Baker and Hammel (1962,1965); it points out how the excess energy and momentum of plasmoids can be dissipated by Joule heating in the 'walls' of the plasma chamber (and similarly in the conducting ionosphere of the Earth). These experimental results will be discussed in section 2.

The second set of experiments are those of Demidenko *et al.* (1967,1969). They deal with plasma elements decelerated and accelerated in regions where the magnetic field intensity is non-uniform, i.e. where the gradient of B is either positive or negative. These largely unknown experimental results will be reviewed in section 3

2. Non-adiabatic deceleration of a plasmoid : The Baker and Hammel's sets of experiments.

2.1. DESCRIPTION OF THE EXPERIMENTS.

The experiments by Baker and Hammel (1962,1965) consisted of injecting collisionless plasma stream in a vacuum chamber perpendicularly to the direction of a uniform magnetic field, B.

Their first set of experiments showed that the plasma stream conserves a constant velocity equal to its injection velocity provided that the wall of the tank are made of electrically non-conducting material : e.g. glass. When the walls are made of insulating material the plasma stream penetrates freely and unimpaired across magnetic field lines, whatever the value of the magnetic field intensity. The ability to penetrate magnetic field lines is then found to be independent of the value of 'Beta', the ratio between the plasma kinetic pressure and the magnetic energy density.

The ability to penetrate a uniform magnetic field is not either depending of the direction of the diamagnetic field carried by the laboratory plasma elements, at the contrary of what Schindler (1979) has inferred from a theoretical study of ideal MHD and 2-D current filaments of infinite length...

In other words, when the electrical Pederson conductivity transverse to the magnetic field direction is small everywhere along the field lines (i.e. even in the walls of the vacuum chamber), the plasma stream is not refrained from moving across magnetic field lines; in this case, 'magnetic field line tying' resulting from the frozen-in-field theorem (and illustrated by cartoons like that of fig. 1), is not supported by this first set of Baker and Hammel's experiments.

In another set of experiments Baker and Hammel showed that when the walls of the vacuum chamber are coated with good electrically conducting material the plasma stream is slowed down along the direction of injection; the plasma flow is then eventually deflected aside as illustrated in fig. 2. In other words as soon as the plasma gets on field lines which are rooted in conducting walls it is decelerated until its forward velocity eventually drops to zero.

(Note that there is no externally imposed electric field in none of these experiments.)

Although, the local plasma density and magnetic field intensity are similar in the vacuum chamber for both sets of experiments, the plasma bulk velocity (or convection velocity) is constant in the first case, while it is decelerated in the latter one; the different conducts come from the different (non-local) boundary conditions : in the first case the electrical conductivity transverse to the magnetic field lines is everywhere nil or almost; in the second case there is a 'weak place' (i.e. the walls) where conductivity is high.

2.2. THE PHYSICAL EXPLANATION

The explanation of the different behaviour of the flow velocities in both sets of experiments is illustrated in fig.3, showing plasma streaming across a uniform magnetic field. The electrons and ions are deflected in opposite directions by the Lorentz force, $q\,\mathbf{v} \times \mathbf{B}$; as a consequence, a net positive charge density builds up along the upper boundary of the injected plasma stream, while a slight excess of electrons forms a negative surface charge density on the opposite side. These surface polarisation charges continue to grow until the resulting charge separation electric field is strong enough to cancel the deflecting effect the magnetic field; i.e. until the electric field intensity measured in the frame of reference co-moving with the plasma is equal to zero : $\mathbf{E}' = \mathbf{E} + \mathbf{v} \times \mathbf{B} = 0$.

In the laboratory frame of reference the polarisation electric field, $\mathbf{E} = -\,\mathbf{v} \times \mathbf{B}$, is precisely equal to what is required for the plasma inside the stream to keep its velocity constant, i.e. equal to its injection velocity, $\mathbf{v}_0$. The plasma stream then continues to move across the magnetic field with the well known $\mathbf{E} \times \mathbf{B}$ drift : $\mathbf{v} = \mathbf{E} \times \mathbf{B} / B^2$. Since the plasma is collisionless, its transverse Pederson conductivity is nil; there is then no way to discharge the electric potential differences set up by the plasma dynamo via local Pederson currents.

In the foremost section of the vacuum chamber where the plasma stream moves across the non-conducting part of the vacuum tank (see fig. 3) the transverse electric potential differences cannot be discharged by electric currents within the walls since they are insulating ones. Therefore, the convection electric field created by the plasma itself is not short circuited, and consequently the stream velocity remains constant.

This is not quite the case in the second portion of the vacuum tank (see fig. 3) where depolarizing currents can flow within the conducting walls; this short circuits the potential differences set up in the plasma stream and distributed on the walls. Note that magnetic field lines are almost equipotentials in collisionless plasmas because the field-aligned conductivity is large, but the local Pederson conductivity is very small within the plasma cloud itself. The convection electric field being short circuited by depolarisation currents in the walls, the plasma bulk speed is reduced until its forward momentum vanishes, somewhat like that of a rain drop falling into a viscous fluid. The initial kinetic energy of the plasma element is dissipated into Joule heating in the walls; its excess initial momentum is also transferred to the walls.

2.3. ADDITIONAL EFFECTS

This simple picture is subject to further refinements.
For example, the particles in the surface charge layers will experience less electric force and consequently cannot keep up with the drift of the main stream : an effect which has been described by Dolique (1963). The 'peeled-off charges which are left behind can provide a source of electric field for the plasma in the wake behind the plasmoid.

Another secondary effect is that the space charge repulsion in the charge layers will spread the polarisation charges laterally along the magnetic field lines, removing particles from the initial stream (Baker and Hammel, 1965). Thus the plasma stream has a tendency to spread along the field lines (Harris et al., 1957).

This is also the place to mention that electrostatic double layers form at the edges of plasmoids where magnetic field lines traverse the surface of the plasmoid. This sets up the appropriate electrostatic potential differences to avoid that the flux of electrons running out of the cloud along magnetic field lines, becomes larger than the escaping flux of the heavier positive charges. Indeed, without such a retarding potential the plasmoid would lose its electrons faster than its ions and become positively charged.

Furthermore, when the diamagnetic plasma stream penetrates the external magnetic field, magnetic probes placed in the vacuum chamber indicate a decrease of **B** (Baker and Hammel, 1962). The time variation of the local magnetic field intensity as measured in the laboratory frame of reference, depends on 'Beta', the ratio between the kinetic and magnetic pressures inside the plasma. However, when Beta is small the diamagnetic currents and the associated magnetic field perturbations are small. In this case the local time derivatives of the **B** are small also.

Note that time derivatives of the local magnetic field intensity generate induced electric fields in the vicinity of the moving plasmoid. It is the importance of these induced electric fields in high-beta plasma, that has been emphasized by Heikkila (1982).

2.4. APPLICATION TO THE MAGNETOSPHERE

How do the Baker and Hammel series of experiments relate to the problem of the solar wind interaction with the Earth's magnetosphere?

The conducting Earth's Ionosphere corresponds to the walls in the last section of the tank where plasma elements are slowed down; the magnetic field lines at the interface between the conducting and insulating sections in fig.3 correspond to the geomagnetic field lines which are tangent to the magnetopause; on one side the magnetic field lines are rooted in the dayside cusps ionosphere and have a relatively large integrated Pederson conductivity; while on the other side of the magnetopause they hang into the solar wind and are rooted in the distant solar atmosphere ; the integrated Pederson conductivity of interplanetary magnetic field lines is much lower.

The injected plasma elements of Baker and Hammel experiments correspond to impinging solar wind plasma irregularities (or plasmoids) which are almost always observed in the magnetosheath. From high resolution plasma and magnetic field measurements it can be inferred that similar plasma irregularities are also present in the solar wind beyond the bow shock. Radio scintillation observations from the corona and solar wind confirm also that during solar active periods the amplitude of these plasma density irregularities is enhanced.

Those plasmoids with larger momentum densities penetrate deeper into the magnetospheric boundary layer than those with a momentum smaller than the average solar wind plasma flow. While the former will be able to penetrate across closed geomagnetic field lines, the latter will be deflected aside in the middle of the magnetosheath without even having been able to reach the magnetopause surface.

The large peak in the ionospheric temperature distribution observed by Titheridge (1976) at the feet of dayside cusp field lines from below 400 km altitude up to 1000 km has been attributed to Joule dissipation of the solar wind plasmoids continuously raining into the magnetosphere (Lemaire and Roth, 1976).
Note however that part of this peak in the ionospheric temperature may also been attributed to elastic collisions of impulsively injected magnetosheath particles precipitating in the upper ionosphere along polar cusp field lines.

The observed poleward motion of ionospheric plasma over the polar caps (Goertz, *et al.*, 1985), as well as recently observed poleward motion of polar cusp auroral features (Sandholt,*et al.*,1985) have been attributed to the momentum transfer of impulsively penetrating solar wind plasmoids in the frontside magnetosphere (Lemaire, 1977, 1987)
Heikkila *et al.*(1988) also emphasize that these moving structures should not be considered as unilateral evidence in favour of patchy reconnection or FTE's. Indeed, these same 'events' (or these same plasma structures) can indeed easily be explained in the framework of Impulsive Penetration Theories.

Since the solar wind is generally a high-beta plasma, the penetrating plasmoids produce large localized diamagnetic field perturbations similar to the magnetic field perturbations observed in Baker and Hammel's experiments.

A video film presented at this NATO Workshop by the author illustrates how diamagnetic fields carried by solar wind plasmoids change the local geomagnetic field distribution in a time dependent manner.

2.5. ADDITIONAL REMARKS

Another lesson that the experiments of Baker and Hammel tells us is that the local magnetic field intensity, the local plasma density distribution and the local pressure distributions within the vacuum chamber don't uniquely determine the bulk velocity of the plasma flow injected into it. Distant (non-local) boundary conditions in the walls (i.e. in the ionosphere) eventually determine the allowed plasma flow patterns, simply by imposing unavoidable constrains to the convection electric field.

Therefore, solving local hydromagnetic transport equations to determine the plasma flow in the distant magnetosphere and in the vicinity of an X-line, without specifying the boundary conditions in the 'walls' (or without giving the distribution of the integrated Pederson and Hall conductivities along magnetic field lines) appears a rather academic exercise, and has limited application to the dissipative magnetosphere-ionosphere system...

Unfortunately in many papers on magnetospheric convection, reconnection and merging, these non-local boundary conditions are not given explicitly; the implicit assumption being that the integrated Pederson conductivity is either equal to zero, or, in other cases (e.g. convection in the plasmasphere) that it is assumed to be infinitely large!...

3. Adiabatic deceleration of a plasmoid : The Demidenko *et al.*'s experiments.

In the previous section we have examined laboratory experiments for which the external magnetic field distribution was uniform. In this section we recall the results obtained in the sixties when plasmoids are injected in a non-uniform magnetic field (Demidenko *et al.*, 1966, 1969, 1972).

3.1. EXPERIMENTAL RESULTS

The magnetic field intensity is parallel to the Oz-axis and perpendicular to the Ox-axis along which the plasmoids are injected with a velocity v_{0x}. The magnetic field intensity varies as a function of x as indicated in fig.4. It increases from a small value at the entry of the vacuum chamber to a maximum value B_0 in the centre; beyond the central point the external magnetic field intensity decreases to a vanishinly small value at the opposite end of the drift tube. No electric field is applied from the outside; however, as in the experiments of Baker and Hammel a polarization electric field , $E_y(x)$, develops naturally within the plasma, as a result of the deflections in opposite directions of the electrons and ions in the magnetic field.

The experiments by Demidenko *et al.* have shown that the velocity inside the plasmoid decreases when it penetrates deeper in the B-field where the intensity becomes larger. The forward bulk velocity $v_x(x)$ satisfies the following relation :

$$v_x = (2/m_p)(W - \mu B_z)^{1/2} \quad (1)$$

where m_p is the ion mass, μ is the mean magnetic moment of the particles and W their mean total energy when they penetrate in the non-uniform magnetic field region :

$$W = m_p v_{0x}^2/2 + \mu B_{0z} \quad (2)$$

$$\mu = k T / B_{0z} \quad (3)$$

Fig.5 shows that the square of v_x is indeed a linear function of the magnetic field intensity B_z, as indicated by equation (1). The slope of the solid line which is a least square fit across the experimental points; its value determines the value of the mean magnetic moment μ which is an adiabatic invariant of motion. The value of B where this straight line cuts the horizontal axis yields the critical field intensity, B_1, where v_x tends to zero.

The distribution of $v_x(x)$ is shown in fig.4 as a function of x. At $x=x_1$, where $B_z=B_1$, the bulk velocity of the plasmoid vanishes because its convection kinetic energy has been entirely transformed into thermal energy. Indeed, as a consequence of conservation of their magnetic moments, the energy associated with the gyro-motion of the particles increases proportionals to the value of B. The perpendicular thermal (gyro-motion) energy increases until the convection (or bulk motion) energy, $m_p v_x^2/2$, has become equal to zero; and this occurs at x_1 where

$$B_z = B_1 = W/\mu \quad (4)$$

At this same distance x_1 the convection electric field

$$E_y = v_x B_z \quad (5)$$

tends also to zero.

The convection electric field inside the plasmoid, $E_y(x)$ has a maximum value at $x=x_2$, where $B=B_2$:

$$B_2 = 2 B_1 / 3 = 2 W / 3 \mu. \quad (6)$$

Furthermore, it has been shown by Demidenko *et al.*(1969) that, as a result of additional drifts in the crossed E_x and B_z fields, there is a variation in the transverse dimension (i.e. along the Oy-axis) of the plasma stream. The width of the stream, h, varies with x according to the relation :

$$h(x)\ E_y(x) = \text{constant}, \quad \text{or}$$

$$h\ v_x\ B_z = \text{constant} \qquad (7)$$

The distribution of h as a function of x is illustrated in fig.4. Note that h(x) has a minimum at $x=x_2$, where the electric field has a maximum. When the front side of the plasmoid approaches the distance $x=x_1$, where v_x tends to zero, the width of the plasma stream tends to spread rapidly in the y-direction, somewhat like the section of a water droplet when it splashes against a solid surface.

From the conservation of particle flux it can also be deduced that the plasma density inside the plasmoid should increase proportionals to the value of B, when it penetrates in the higher field region and approaches x_1.

When the initial total energy W is large enough (i.e. when $W > \mu B_0$), the magnetic barrier is not quite high enough to stop the plasma element completely; beyond $x=x_0$, where the magnetic field intensity has a maximum, the plasmoid is accelerated adiabatically by the negative field gradient.

On the contrary, when the initial total energy W is smaller then μB_0, the plasma stream is stopped and should be reflected adiabatically. But the reflected plasma stream will then interact with the incoming stream; this leads to a cancellation of the polarization electric fields in the opposite directed plasma streams. The kinetic energy associated with the directed particle motion must then be transformed into gyro-motion, with the consequence that the perpendicular temperature increases.

In one dimensional flow system a backward propagating front should in principle appear. Behind this backward propagating wave front more and more heated plasma is piled up against the magnetic barrier. If the incoming plasma has a supersonic injection velocity, like the solar wind, the backward propagating wave front is a shock wave.

However, the distribution of laboratory magnetic fields (and of the geomagnetic field) are not 1-D, but 3-D ones. Therefore, instead of piling up indefinitely against the magnetic barrier, the stream is deflected aside along the flanks and finds a way where the gradient of the magnetic field intensity is smaller.

In all these Controlled Laboratory Experiments of Demidenko *et al.* where adiabatic deceleration and acceleration of plasmoids are investigated, the walls of the vacuum chamber were, of course, made out of glass which is an insulator; this avoids non-adiabatic deceleration resulting from depolarisation wall currents, as in the experiments of Baker and Hammel discussed above.

3.2. THE PHYSICAL EXPLANATION

Some of the experimental results discussed in the previous section had already been predicted theoretically by Schmidt (1960). The reader is conveyed to consult this original contribution, or the paper by Demidenko *et al.*(1967) where the equations (1)-(7) are also derived from first principles. There is no need to repeat, here, this straightforward derivation once more.

Let us just mention that this derivation is based on Poisson's equation and on the equation giving the polarisation current density in a plasma when the electric field intensity changes with time. The validity of this set of equations rests on the assumption that the dielectric constant of the plasma is much larger than unity; this is not only the case in all controlled laboratory experiments discussed above, but this is also always a valid approximation in magnetospheric and solar wind plasmas.

Note also that the results obtained in the first set of Baker and Hammel's experiments can be deduced from equation (1), when the external magnetic field is uniform. Indeed, when B_z is independent of x in equation (1), it can be seen that v^x is then also a constant, as precisely demonstrated experimentally by Baker and Hammel... at least when the walls of the vacuum chamber are coated with insulating material.

3.3. APPLICATION TO THE MAGNETOSPHERE

How do Demidenko *et al.*'s results apply to the study of impulsive penetration of solar wind plasmoids into the Earth's magnetosphere?

The magnetic field distribution corresponding to Demidenko *et al.*'s experiments increases from a small value to higher value without changing direction, just like the B-field at the front side magnetopause when the IMF is due Northward (NB_z IMF), or, along the surface of the magnetotail lobes when the IMF is Southward.

The magnetosheath corresponds to the region where the heated (compressed) solar wind plasma tends to pile up against the geomagnetic barrier, and where eventually it slips aside along the flanks of the 3-D magnetospheric cavity. The point of deepest penetration of an injected plasma element depends of its initial energy W; the value of the magnetic field intensity where its forward bulk velocity eventually vanishes is given by equation (4).

From the r^{-3} radial distribution of the geomagnetic field distribution it can be determined that the average solar wind plasmoids with an average momentum flux density should be stopped or deflected at about 10 Earth's radii in the sunward direction : i.E. at the average magnetopause position.

But a very large momentum flux density is required in the solar wind to obtain from equation (4), a value for B_1 which is equal to the geomagnetic field intensity at geostationary orbit. Therefore, it is only on very rare occasions that solar wind plasma elements will be able to penetrate as deep as 6.6 Earth's radii.

The plasmoids with the largest momentum flux density will penetrate deepest in the geomagnetic field, where they produce localized diamagnetic field perturbations, magnetosheath like plasma density enhancements, as well as localized electric field perturbations; these small scale and time-dependant electric fields perturbations produce convection in the ambient magnetospheric plasma along the flanks of the penetrating plasmoids as illustrated in fig.6. The external magnetospheric plasma is then pushed aside.

It has already been mentioned above that these small scale magnetospheric convection patterns driven by impulsively injected plasmoids map down in the dayside cusp ionosphere, where they have been observed as localized poleward moving ionospheric irregularities or auroral features (Goertz, *et al.*, 1985, Sandholt, *et al.* 1985, Glassmeier, *et al.*,1988, Friis-Christensen, *et al.*, 1988, Lanzerotti, 1989, Heikkila, *et al.* 1988).

Any plasma density irregularity which impacts on the Bow Shock with a momentum flux density smaller than the average solar wind value is not able to reach the average magnetopause position where 'average' plasmoids are stopped and deflected.

3.4. ADDITIONAL COMMENTS

Of course the IMF is rarely due Northward or Southward, generally it is at an angle between 0 and 180 degrees with respect to the direction of the geomagnetic field. In this case the eqs.(1) to (7) can be generalized and extended (see Lemaire, 1985). It would be most interesting to modify the magnetic field distribution from Demidenko *et al.*'s experiment to simulate this more general situation when the IMF is not aligned with the Northward geomagnetic field, i.e. when the magnetic field is sheared as usually near the magnetopause.

4. Discussion and conclusions.

There are several other plasma laboratory experiments whose results are published in technical Journals, and, which are relevant to our understanding of Solar Wind Magnetosphere Interaction (see for instance Fälthammar ,1988).

Let us mention for instance those results obtained by Bostick

(1956) with two interacting plasmoids moving in opposite directions against each others. These experiments may illustrate the dipole-dipole magnetic interaction between two plasmoids; indeed the current systems carried by plasmoids have dipole moments which can have a different orientation from the neighbouring one; consequently, as a result of the dipole-dipole interaction both plasmoids can be either attracted or repelled.

Bostick's type of experiments may be of great importance for those who are interested in the dipole-dipole interaction between interplanetary plasmoids and magnetospheres. Indeed, the magnetosphere is a huge plasmoid with a large dipole moment; it has been suggested by Lemaire (1985, 1987) that the magnetic dipole-dipole interaction between the Earth's dipole moment and that of the penetrating plasmoid (whose orientation is dependent of the ambient IMF direction) controls, to a certain extend, impulsive penetration of solar wind plasma elements into the magnetosphere (see also, Lemaire *et al.*, 1987).

Other experiments like that of Lindberg (1978) should also be mentioned as most relevant to the study of the solar wind magnetosphere interaction. Indeed, it may simulate solar wind plasma injected along the curved magnetic field lines of the dayside clefts.

These controlled laboratory plasma experiments could be reinstated and extended at relatively low cost. New types of experiments could also be imagined to enhance our current incomplete understanding of the interaction between the solar wind and the magnetosphere, e.g. the phenomenon of filamentation or breaking-off of plasmoids into separated entities when they penetrate into a non-uniform magnetic field like the geomagnetic field.

Moreover, experimental results always remain the test-bench for any theory even the most appealing and popular ones : the most careful referee will never replace a carefully conducted experimental test...

New breeds of controlled laboratory experiments could be most valuable to improve our current understanding of **'non-anomalous'** interaction mechanisms between the **non-uniform and non-steady** state solar wind plasma and the Earth's Magnetosphere.

LIST OF REFERENCES

Axford W.I. and Hines C.O., Can. J. Phys., 39, 1433, 1961.

Baker, D.A. and Hammel, J.E., Phys. Fluids, 8, 713,1965.

Baker, D.A. and Hammel, J.E., Phys. Rev. letters, 8, 157-158, 1962.

Bostick, W.H., Phys. Rev., 10, 292-299, 1956.

Demidenko, I.I., Lomino, N.S., Padalka, V.G., Rutkevitch, B.N.,, and Sinel'niko, K.D., Soviet Physics - Technical Physics, 14, 16-22, 1969.

Demidenko, I.I., Lomino, N.S., Padalka, V.G., Soviet Physics - Technical Physics, 16, 1096-1101 , 1972.

Demidenko, I.I., Lomino, N.S., Padalka, V.G., Safranov, B.G., and Sinel'niko, K.D., J. Nucl. Energy, C, Plasma physics, 8, 433, 1966.

Demidenko, I.L., Lomino,N;S., Padalka, V.G., Rutkevick, B.N. & Sinel'nikov, K.D., Soviet Phys. Techn. Phys., 11, 1354, 1967.

Demidenko, I.L., Lomino,N;S., Padalka, V.G., Rutkevick, B.N. & Sinel'nikov, K.D., Soviet Phys. Techn. Phys., 14, 16, 1969.

Dolique, J.M., Compt. Rendus, 256, 4170, 1963.

Dungey J.W., Phys. Rev. Lett., 6, 47, 1961.

Fälthammar, C.-G., Laser and Particle Beams, 3-3, 437-452, 1988.

Friis-Christensen, E., McHenry, M.A., Clauer, C.R. and Vennerstrom, S., Geophys. Res. Lett., 15, 253, 1988.

Glassmeier, K.-H., Hoenisch, M., and United, J., J. Geophys. Res., 1988

Goertz, C.K., Nielsen, E., Korth, A., Glassmeier, K.H., Haldoupis, C., Hoeg, P., and Hayward, D., J. Geophys. Res., 87, 2147-2158, 1985.

Harris, E.G., Theus, R.B., and Bostick, W.N., Phys. Rev., 105, 46, 1957.

Heikkila W.J., Geophys. Res. Lett. 9, 877, 1982.

Heikkila W.J., Planet. Space Sci., 26, 121, 1978.

Heikkila W.J., Jorgensen, T.S. and Lanzerotti, L., A transient auroral event on the dayside, preprint, 1988.

Lanzerotti, L.J., Advances in Space Research, in press 1989.

Lemaire J. and Roth M., J. Atmospheric and Terr. Phys., 40 331-335, 1978.

Lemaire J., Planet. Space Sci., 25, 887-890, 1977.

Lemaire, J., Interpretation of the Northward Bz (NBZ) Birkeland current system and polar cap convection patterns in terms of the impulsive penetration model, in Magnetotail Physics, Ed. A.T.Y. Lui, Johns Hopkins University Press, pp 83-90, 1987.

Lemaire, J., J. of Plasma Physics, 33, part 3, 425-436, 1985.

Lemaire,J., Rycroft, M.J., and Roth, M., Planet. Space Sci., 27, 47-57, 1979.

Lindberg, L., Astrophys. and Space Sci., 55, 203-225, 1978.

Linhart, J.G., 'Plasma Physics', North Holland Publ. Co., Amsterdam, p 157-160, 1960.

Lundin, R. and Dubinin, E., Planet. Space Sci., 32, 745-755, 1984.

Lundin, R., Stasiewicz, K., and Hultqvist, B., J. Geophys. Res., 92, 3214-3222, 1987.

Russell, C.T. and Elphic R.C., Space ScI. Rev., 22, 681, 1978.

Sandholt, P.E., Egeland, A., Lybekk, B;, and Deehr, C.S., Signature of flux transfer events in the dayside aurora? preprint, University of Oslo, 1985.

Schindler, K., J. Geophys. Res., 84, 7257-7263, 1979.

Schmidt, G., Phys. Fluids, 3, 961, 1960.

Sckopke, N., Paschman, G., Haerendel, G., Sonnerup, B.U.O., Bame, S.J., Forbes, T.G., Hones, E.W.,Jr., and Russell, C.T., J. Geophys. Res., 86, 2099, 1981.

Titheridge, J.E., J. Geophys. Research, 81, 3221, 1976.

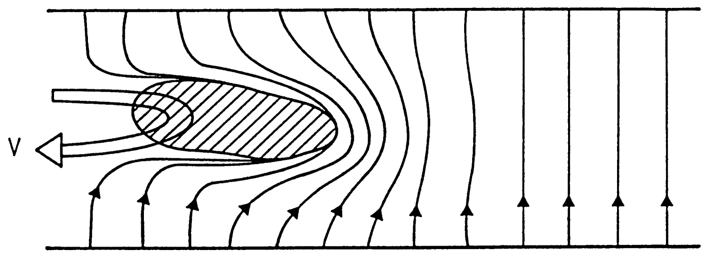

Fig. 1 Cartoon commonly drawn to illustrate magnetic field line tying, and reflection of a collisionless plasma element penetrating into a magnetic field.

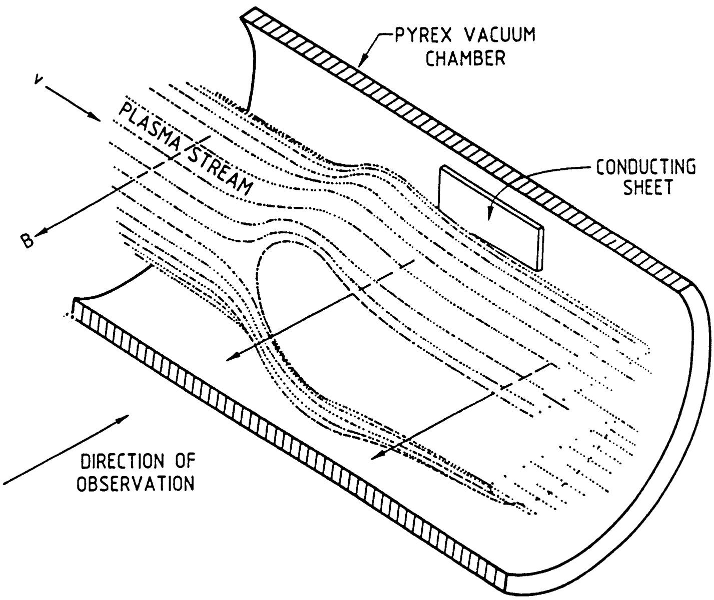

Fig. 2 Schematic diagram of a plasma flow around the cylindrical region of zero electric field created by a conducting strip located adjacent to the inside wall of the vacuum chamber. (after Baker and Hammel, 1962)

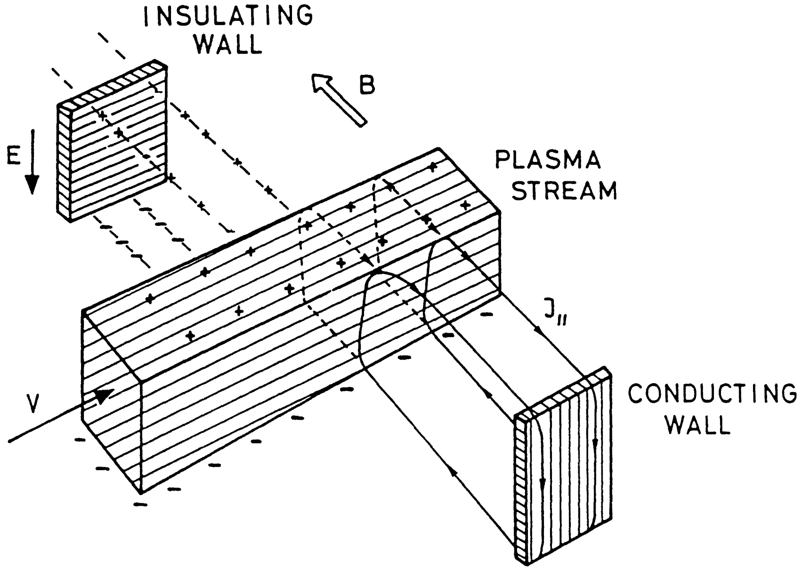

Fig. 3 Simplified model of a collisionless plasma flow crossing a uniform magnetic field showing (i) the charging up effect of an insulating wall and (ii) depolarizing effect of a conducting wall. (after Baker and Hammel, 1965)

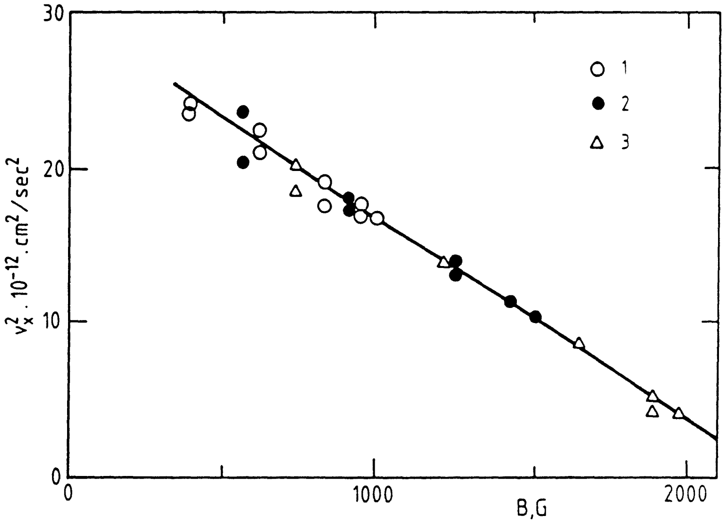

Fig. 4 Adiabatic deceleration of a plasmoid in a region of increasing magnetic field intensity. Distribution as a function of x, the distance along the injection axis of a plasmoid in a non-uniform magnetic field whose intensity is parallel to the Oz-axis and whose intensity is given by the curve labelled B(x).The bulk velocity, v_x, and the width in the Oy direction, h(x), are also given. (after Demidenko, *et al.*, 1972)

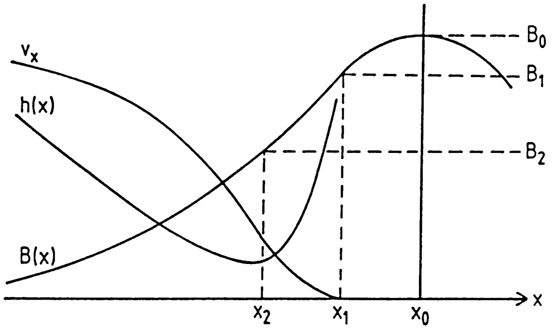

Fig. 5 Adiabatic deceleration of a plasmoid in a region of increasing magnetic field intensity. The square of the bulk velocity of the plasmoid is given as a function of the intensity of the magnetic field. The experimental points correspond to three different magnetic field profiles for a peak magnetic field intensity of (1) B_o = 1000 G ; (2) 1500 G ; (3) 2000 G. (after Demidenko, *et al.*, 1969)

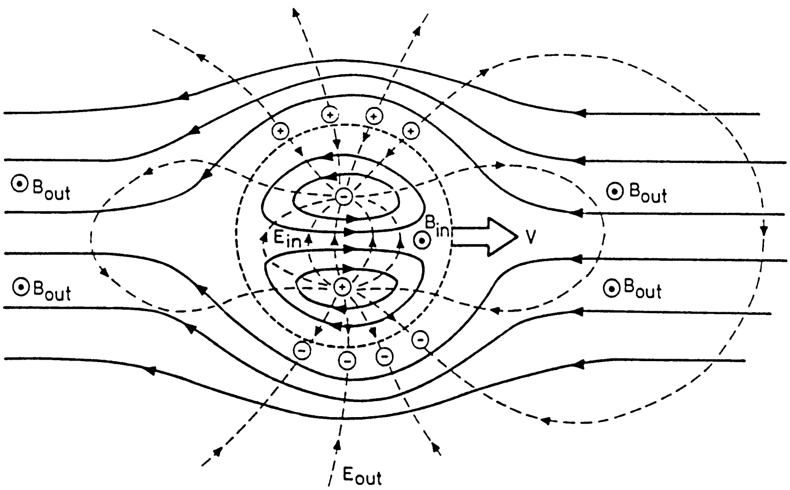

Fig. 6 Cartoon illustrating possible flow of external plasma around a penetrating plasmoid. Possible plasma flow pattern inside the plasmoid is also suggested.